Int. J. Heat Mass Transfer. Vol. 36, No. 10, pp. 2565–2573, 1993
Printed in Great Britain

0017–9310/93 $6.00 + 0.00

Transient method for measuring thermal properties of saturated porous media

OSVAIR V. TREVISAN
Faculdade de Engenharia de Campinas, Universidade Estadual de Campinas, 13081 Campinas SP, Brazil

and

SITAKANTA MOHANTY and MARK A. MILLER
Department of Petroleum Engineering, University of Texas at Austin, Austin, TX 78712, U.S.A.

(*Received* 27 *July* 1992 *and in final form* 25 *November* 1992)

Abstract—This paper describes the development of a transient technique to measure thermal diffusivity and conductivity of porous samples. The method uses the film heat sensor to probe heat flux. Temperature and heat flux are measured dynamically allowing conditions to vary in time at the point of measurement. The data are then treated by a deconvolution algorithm, rendering results proper to simpler models for the same geometry. The numerical treatment in the deconvolution procedure was verified for a hypothetical case. The method was finally tested in the laboratory, with experiments made on samples of natural rock.

INTRODUCTION

HEAT TRANSFER properties of porous media containing fluids constitute the most basic input for thermal engineering calculations in several fields. Knowledge of these properties is definitely required for the design and evaluation of thermal methods of oil recovery. It is often needed in applications as diverse as insulation design, food processing, geothermal engineering and in fundamental studies in soil science, geophysics, to name a few. Many numerical and analytical models are available for the evaluation and analysis of the several thermal related processes involved in those areas. Models have been developed to take into account several different aspects of the heat transfer physics. The common ground is that the great majority of these models are indistinctly based upon well defined, well-characterized physico-chemical properties. The usual, implicitly assumed premise is that physical properties can be measured as precisely as demanded, either in the labs or in the field. In this sense, all models depend on accurate and correct measurements of the characteristic properties to render meaningful results. This is even more crucial as engineers and scientists progress towards more refined models.

The apparatus depicted in Fig. 1 is an equipment designed for measurements of thermal conductivity and diffusivity in cores extracted of oil bearing formations. Intended for both steady and unsteady measurement methods, the cell can accommodate rock samples of 3.81 cm in diameter by 2.54 cm long. The design allows one to vary the saturation of multiphase fluids at different temperature levels up to 232°C. In order to avoid fluid vaporization at higher temperatures, the cell is built to hold external pressures of up to 28×10^5 Pa. Regarding heat loss prevention, the design follows the guarded hot plate idea. The heat source is surrounded by a guard ring to force heat from the source to flow axially through the sample. The guard heater temperature is controlled independently. A separate electrical system controls the heat supply to maintain both the heat source and the guard heater at the same temperature. The equipment differs from a standard guarded hot plate by the sleeve encapsulating the sample, necessary to confine the specimen under pressure. More details on the apparatus can be found in ref. [1].

HEAT SENSORS

Most experiments held in the heat transfer area use only thermocouples or resistance temperature detectors (RTD), and only temperature is measured as a primary variable. Heat flux is rarely measured. Being an important quantity for most thermal engineering purposes, the heat flux is usually calculated or inferred from the temperature distribution across the system. When the energy balance permits, the heat flux can also be calculated from measurements of external energy inputs to the thermal system.

The measurement of heat flux can become an essential task, as in the methodology proposed in this work. The thin film technology presents good potential to meet the requirements of a fast-response, low thermal resistance, low interference technique. As in most techniques, the amount of heat flux is determined by the heat conduction between two points. It basically requires the temperature difference and the thermal resistance between the two points to be known. The

NOMENCLATURE

A	cross-sectional area
K	conductivity
L	length
q	heat flux
q_r	reference heat flux
s	Laplace variable
t	time
T	temperature
x	Cartesian coordinate.

Greek symbols

α	thermal diffusivity
β	angular coefficient
θ	dimensionless temperature
Θ	dimensionless temperature
Ψ	solution for unity temperature at the boundary
Ω	solution for unity heat flux at the boundary.

Superscripts and subscripts

$( )^*$	dimensionless variable
$(\bar{\ })$	quantity in Laplace space
$( )_i$	initial condition
$( )_0$	at the boundary.

heat sensor is made with a thin plastic film of very well and accurately determined conductivity. The sensor determines the heat flux by measuring the temperature difference across the film. A number of thermocouple pairs are assembled on each side of the film, so that the thermoelectric junctions on one side directly face those on the other side (see Fig. 2). Due to the small temperature difference across the film—the difference

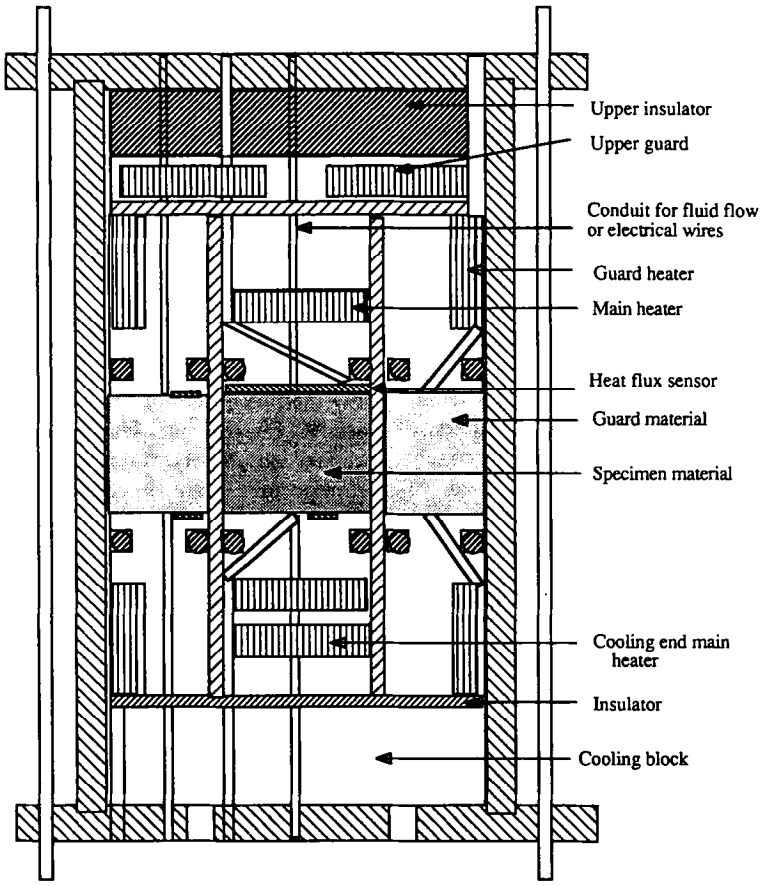

FIG. 1. Schematic of the experimental apparatus.

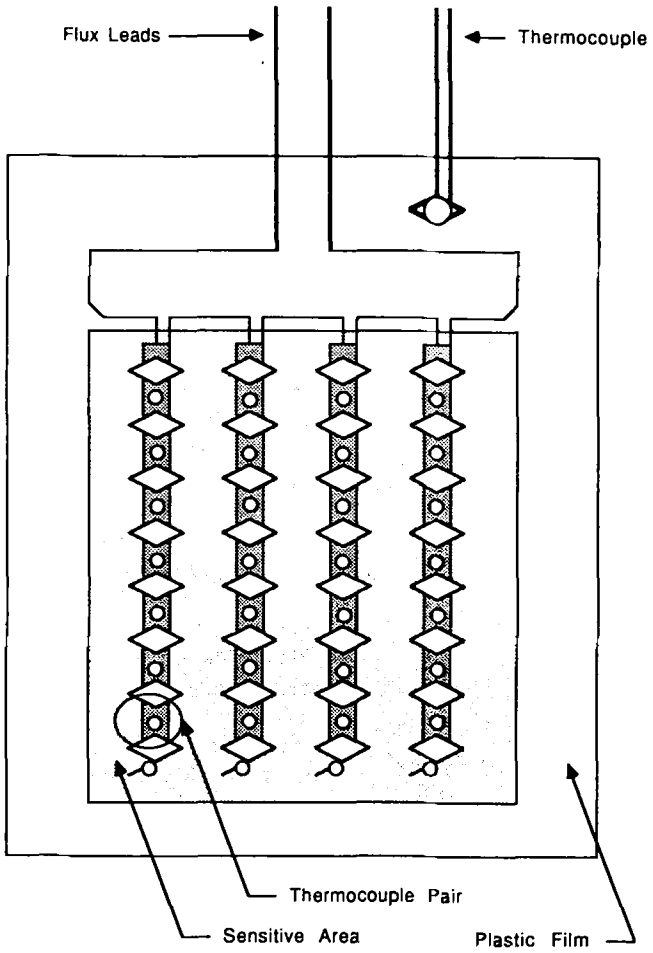

FIG. 2. Heat flux sensor.

is obviously directly dependent upon the plastic conductivity and film thickness—the thermocouples are electrically connected to provide a detectable voltage signal at the output. As in the case of thermocouples, the voltage difference is proportional to the temperature difference across the plastic layer and therefore to the heat flux crossing the layer. The sensor selected to carry out the experiments of the present work is the RdF 20457-2 sensor. The reasons for choosing this sensor were basically the very low thermal resistance presented by the probe, the small size aspect of the sensitive area (which makes the sensor extremely appropriate for laboratory use) and the thermal capacity—response time low range of the complete set. The sensitivity, which is associated with the number of thermocouple pairs embodied in the sensor, was the parameter to sort out the series offered by the manufacturer. The criterion used to pick the model in the series was the product of thermal capacity and response time. The nominal characteristic values for the model chosen are, as translated from the data furnished by the manufacturer:

sensor	RdF model 20457-2
sensitivity	1.05 μV W^{-1} m^{-2}
response time	0.060 s
thickness	0.15 mm
thermal capacity	0.41 kJ K^{-1} m^{-2}
thermal conductance	0.0284 W K^{-1} m^{-2}
number of pairs	40.

TRANSIENT METHOD

Experimental methods used to determine thermal conductivities of materials can be classified into two major categories: (1) steady state methods and (2) transient methods.

The most distinctive feature between the two categories is the variation in time of the temperature distribution. Transient methods involve the complete differential equation for heat flow, where time and space are both considered. As conduction problems present first a non-steady regime, steady-state methods must guarantee that the transient period has ended. So, in contrast to transient methods, steady-

state techniques require long periods to be realized. The short-time advantage of the transient methods places the burden on the demand for very accurate and rapidly responding instruments. On the other hand, heat losses have a smaller influence when measuring times are shorter—relieving transient methods of the struggle to eliminate all accounted and non-accounted heat losses.

Thermal conductivity is determined in steady state procedures from the measurement of two quantities: (1) the heat flux crossing a unidimensional specimen and (2) the temperature difference between two points along the specimen. The heat flux is usually determined from a heat balance over the sample. One strong reason to wait until the steady state regime settles is to avoid energy accumulation in the sample or metering blocks, which would be one more source of error in the energy balance. The other major concern with making the appropriate heat balance is related to the heat losses. Most of the discussion of steady state procedures has been about methods to prevent and methods to properly account for heat losses.

In the specific category of transient methods, several techniques have been proposed [2]. The profusion of methods is related to the diversity of configurations, materials and applications of heat conduction. Methods have differed by the geometry of specimens and by the boundary conditions imposed on them. Examples of the richness of the field are the collection of periodic temperature techniques and plain transitory methods. They have been applied on rods, long rods, flat plates, semi-infinite solids, spheres and others. Some of these methods also are branched out by procedures used to prevent or to account for heat losses. Most of the transient techniques are based only on temperature measurements and for this reason are bounded to the determination of diffusivity only.

In order to determine conductivity the heat flux must be measured or determined from independent data. The experimental procedure to fulfill this need has traditionally been to place a constant heat source at a convenient boundary. The heat flux is then measured by the electrical power input to the heat source, implicitly assuming that the heater has negligible heat capacity, that there are no heat losses through edges or wires. Unidimensional conduction also requires that the constantly generated heat is evenly distributed over the heater sample contact area. The temperature changes associated with the heat input are measured either at the same boundary [3] or at a certain depth into the sample [4].

The method proposed in this study can also be classified in the transient category. It uses the thin film sensor technology to measure the heat input into the sample. The thin film technology has only recently gained attention from scientists and engineers [5] and to our knowledge is used for the first time to evaluate thermo-physical properties of materials. The heat sensor is able to measure dynamically varying heat inputs. Along with the temperature readings by thermocouples, which also permit time variation, these data form the history of the test. The data treatment involves deconvolving the temperature and heat flux as functions of time, so that simpler models can be generated for the same physical configuration. This method presents important advantages over other transient methods, the most important being:

(1) There is no restriction on the heat capacity of the heating source, as the heat is measured right at the interface where it is needed to be known.

(2) There is no need to insert probes inside the sample, so avoiding the common problems observed in this action, such as poor thermal contact and physical alterations caused by machining operations.

(3) There is no need to guarantee specific boundary conditions at the measuring surface, such as constant heat input or constant temperature.

(4) The possibility of measuring one more characteristic (besides diffusivity), if the experiment is run long enough.

(5) Although not intended to substitute steady state methods in the determination of conductivity in long term experiments, the proposed method is particularly useful in situations where long term heat transfer occurs also at dynamically varying conditions.

ANALYSIS

The heat transfer across a one-dimensional slab is governed by the differential equation

$$\frac{\partial^2 T}{\partial x^2} = \frac{1}{\alpha}\frac{\partial T}{\partial t} \tag{1}$$

where α = thermal diffusivity of the medium, T = temperature and t = time. The entire sample (slab) is initially at a homogeneous temperature

$$t = 0 \quad T = T_i. \tag{2}$$

The temperature at the cool end of the sample is maintained constant

$$x = L \quad T = T_i. \tag{3}$$

The boundary condition at the heated surface involves variations of both heat flux and temperature.

$$x = 0 \quad KA\frac{\partial T}{\partial x} = q_o(t)$$

$$x = 0 \qquad T(0) = T_o(t). \tag{4}$$

These two quantities, known from the measurements in the experimental procedure, are not independent. They are related to each other by a function of the parameters we want to determine, namely, the diffusivity and the conductivity of the sample material. One way to disclose the relation between $q_0(t)$ and $T_0(t)$ is to examine the two following independent problems.

Problem I—known temperature at $x = 0$

$$\frac{\partial^2\theta}{\partial x^{*2}} = \frac{\partial\theta}{\partial t^*} \tag{5}$$

$$t^* = 0 \quad \theta = 0$$

$$x^* = 0 \quad \theta = \theta_o(t^*)$$

$$x^* = 1 \quad \theta = 0 \tag{6}$$

which is the non-dimensional version of the problem, after substituting the non-dimensional variables

$$x^* = \frac{x}{L}$$

$$\theta = \frac{T - T_o}{\frac{q_r L}{KA}}$$

$$t^* = \frac{t\alpha}{L}$$

$$q^* = \frac{q}{q_r}. \tag{7}$$

The solution to equations (5)–(7) can be given by

$$\theta = \int_0^{t^*} q_o(t^*)\frac{\partial\Omega}{\partial t^*}(t^* - t)\,dt \tag{8}$$

where Ω is the solution of the same problem when $\theta_o(t^*) = 1$.

Problem II—known heat flux at $x = 0$

$$\frac{\partial^2\Theta}{\partial x^{*2}} = \frac{\partial\Theta}{\partial t^*} \tag{9}$$

$$t^* = 0 \quad \Theta = 0$$

$$x^* = 0 \quad \frac{\partial\Theta}{\partial x^*} = q_o^*(t^*)$$

$$x^* = 1 \quad \Theta = 0. \tag{10}$$

The solution in this case is given by

$$\Theta = \int_0^{t^*} q_o^*(t^*)\frac{\partial\Psi}{\partial t^*}(t^* - \tau)\,d\tau \tag{11}$$

Ψ being the solution to the problem with $q_o^*(t^*) = 1$. In Laplace space, the basic solutions Ω and Ψ are given by

$$\bar{\Omega} = \frac{\sinh[(1 - x^*)\sqrt{s^*}]}{s^*\sinh(\sqrt{s^*})} \tag{12}$$

$$\bar{\Psi} = \frac{\sinh[(1 - x^*)\sqrt{s^*}]}{s^*\sqrt{s^*}\cosh(\sqrt{s^*})}. \tag{13}$$

Also the convolution integrals of equation (8) and equation (11) can be expressed by

$$\theta = \overline{\theta_o}\, s^*\bar{\Omega} \tag{14}$$

and

$$\Theta = \overline{q_o^*}\, s^*\bar{\Psi}. \tag{15}$$

Recalling that Problems I and II are two different interpretations of the same physical problem, in other words, $\theta = \Theta$

$$\frac{\overline{\theta_o}}{\overline{\overline{q_o^*}}} = \frac{\bar{\Psi}}{\bar{\Omega}} \tag{16}$$

or

$$\frac{\overline{\theta_o}}{\overline{\overline{q_o^*}}} = \frac{\tanh(\sqrt{s^*})}{\sqrt{s^*}}. \tag{17}$$

The limit for small values of $s^*(t^* \to \infty)$ of the previous function is

$$\lim_{s^* \to 0}\left(\frac{\overline{\theta_o}}{\overline{\overline{q_o^*}}}\right) = 1. \tag{18}$$

While for large values of s^* (small t^*)

$$\lim_{s^* \to \infty}\left(\frac{\overline{\theta_o}}{\overline{\overline{q_o^*}}}\right) = \frac{1}{\sqrt{s^*}}. \tag{19}$$

Figure 3 shows the characteristic curve of the functions in equation (16) vs s^* in a log–log plot. At the range of large s^* values the curve turns to a straight line of slope $-(1/2)$, corresponding to the transient period of heat conduction. The steady state regime is characterized by the flat portion of the curve. A type curve match could be used by taking the plot of Fig. 3 as the type curve to verify the transition between regimes and to estimate both parameters of conductivity and diffusivity. The scale on the vertical coordinate of the real data plot would be $(\overline{T_o - T_i})/\overline{q_o}$, which is related to the corresponding scale of the type curve by

$$\frac{(\overline{T_o - T_i})}{\overline{q_o}} = \frac{L}{KA}\left(\frac{\overline{\theta_o}}{\overline{\overline{q_o^*}}}\right). \tag{20}$$

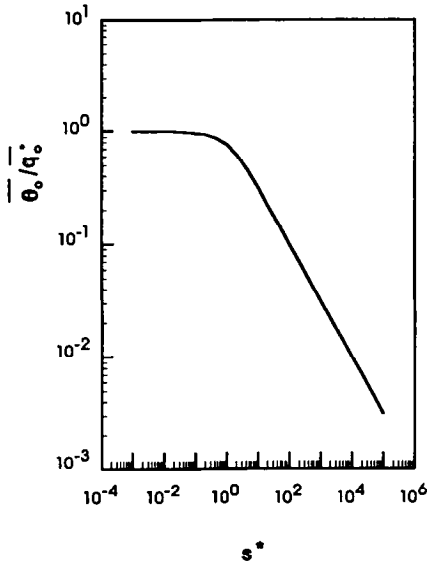

FIG. 3. Type curve for constant heat flux boundary in Laplace space.

Once the steady state plateau on Fig. 3 is reached, the thermal conductivity is determined by

$$K = \frac{L}{A}\left[\frac{\overline{q_o}}{(\overline{T_o - T_i})}\right]. \tag{21}$$

Also from the curve of Fig. 3, the steady state regime is fully established for s^* values lower than 2.5×10^{-1}. In terms of real data calculations the corresponding criterion for s is

$$s = \frac{\alpha}{L^2} s^* < \frac{\alpha}{L^2} \times 2.5 \times 10^{-1}. \tag{22}$$

However, the determination of diffusivity may be obtained from data gathered at earlier times, in other words for higher values of s. This is accomplished by observing that for $s^* \to \infty$

$$\frac{\overline{\theta_o}}{\overline{q_o^*}} = s^{*-1/2} \tag{23}$$

or in terms of dimensional data

$$\frac{(\overline{T_o - T_i})}{\overline{q_o}} = \frac{\sqrt{\alpha}}{KA} s^{-1/2}. \tag{24}$$

The coefficient at the right hand side of equation (24) can be determined from the slope of the plot $(\overline{T_o - T_i})/\overline{q_o}$ vs $s^{-1/2}$. If the slope of the curve is β, then

$$\beta = \frac{\sqrt{\alpha}}{KA}. \tag{25}$$

NUMERICAL TEST

The procedure to determine K and α via equations (21) and (25) involves first recording the time evolution of $(T_o - T_i)$ and q_o since the very beginning of the experiment. The Laplace transform, needed to deconvolute the temperature and heat flux functions, is calculated numerically from both history data. This calculation yields the values necessary to plot a curve similar to Fig. 3. The Laplace transform is obtained by numerically integrating

$$(\overline{T_o - T_i})(s) = \int_0^\infty e^{-st}(T_o - T_i)(t)\,dt. \tag{26}$$

The numerical procedure used in the present work to calculate the integral in equation (26) is based on a Simpson adaptive scheme [6]. Interpolation of data was obtained by a cubic spline method of second order [7]. The upper limit of the integral in equation (26) depend on s and, for the purpose of this work, its numerical value is taken high enough to render no alteration greater than 1×10^{-3} to the integral result.

In order to evaluate the accuracy of the numerical treatment, a test was developed with artificially generated data. As the temperature increase in the early moments is certainly commanded by the thermal inertia of the upper metallic block in the apparatus of Fig. 1, a linear temperature history was assumed to hold at the surface of the sample. If a reasonable temperature difference of 10°C is to be imposed on the sample, the linear increase will be effective until 2000 s given the mass of the upper block. After this time the temperature control system acts to maintain constant temperature at the surface. The temperature history is so described by

$$T_o - T_i = 5 \times 10^{-3} t, \quad t < 2000 \tag{27}$$

$$T_o - T_i = 10, \quad t \geqslant 2000. \tag{28}$$

The heat flux at the surface associated with the imposed temperature increase is calculated from the analytical solution to the problem of heat conduction in a slab [8]. It is obtained by numerically inverting the Laplace transform [9] of

$$\overline{q_o} = \frac{KA}{\sqrt{\alpha}} s(\overline{T_o - T_i}) \frac{\operatorname{cotanh}\left(\frac{L}{\sqrt{\alpha}}\sqrt{s}\right)}{\sqrt{s}} \tag{29}$$

with

$$(T_o - T_i) = \frac{5 \times 10^{-3}}{s^2}(1 - e^{-2000s}). \tag{30}$$

The geometric parameters used to generate the data reflect the apparatus of Fig. 1. The physical properties of the hypothetical sample are taken as representative of oil saturated sandstones. The input values are

$$L = 2.54 \times 10^{-2}\,\text{m}$$
$$A = 8.0 \times 10^{-4}\,\text{m}^2$$
$$\alpha = 1 \times 10^{-6}\,\text{m}^2\,\text{s}^{-1}$$
$$K = 2.5\,\text{W m}^{-1}\,\text{K}^{-1}. \tag{31}$$

Figure 4 shows the artificial data curves taken as input

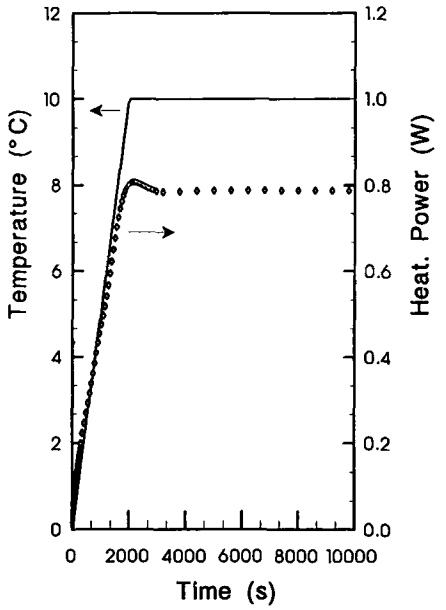

FIG. 4. Simulated history data with $K = 2.5$ and $\alpha = 1 \times 10^{-6}$ (SI).

to the data treatment scheme for obtaining conductivity and diffusivity.

Following the procedure explained in the previous section we were able to reproduce the format of the curve in Fig. 3 as shown in Fig. 5. In this figure the treated data is plotted for discrete values of s. The curve levels off in the small range of s at the value

$$\frac{(\overline{T_o} - \overline{T_i})}{\overline{q_o}} = 12.696\,\mathrm{K\,W^{-1}} \tag{32}$$

yielding, according to equation (21),

$$K = 2.5008\,\mathrm{W\,m^{-1}\,K^{-1}} \tag{33}$$

which is a very accurate reproduction of the value assumed in the data generation process.

The diffusivity is determined by plotting the curve shown in Fig. 6. The slope of the straight line in the figure, determined by linear regression, is

$$\beta = 0.5007\,\mathrm{K\,W^{-1}\,s^{-1/2}} \tag{34}$$

rendering, from equation (25),

$$\alpha = 1.002 \times 10^{-6}\,\mathrm{m^2\,s^{-1}} \tag{35}$$

against the original value of 1.0×10^{-6}. These test results show that the numerical scheme used is very accurate and adequate to treat the data.

EXPERIMENTAL PROCEDURE AND RESULTS

The cell as depicted in Fig. 1 was mounted on a bench with the heaters connected to independent power suppliers. The power supply to the heaters was monitored and controlled by a data acquisition system. Thermocouples were placed near each guard heater, in order to guarantee an even temperature gradient along the axis of the cell. The heat flux and temperature readings were stored in the system at

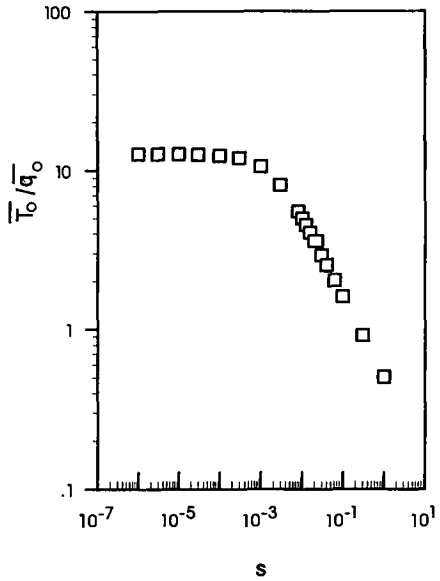

FIG. 5. Constant heat flux solution from deconvolved data.

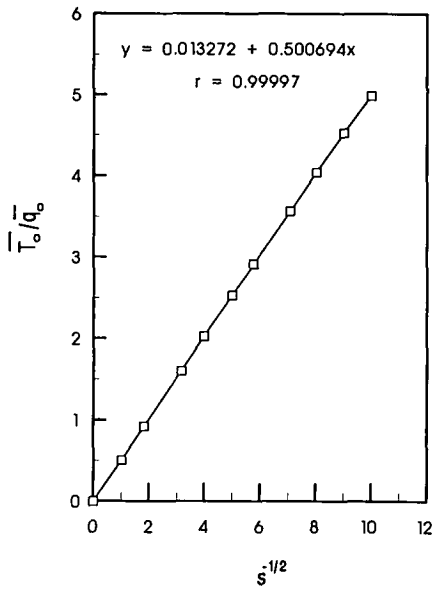

FIG. 6. Early transient solution after data deconvolution.

frequencies that varied through the experiment history. Data collection was more intense at the beginning of the runs, and progressively diminished as time passed. Typically, the readings were recorded every 0.5 s at the first 30 s (starting at the moment the differential heating begins), every 5 s up to 5 min, and then every minute till the end of the run. The temperature at the bottom of the sample was maintained constant by combining the inputs of an electric heater and a coiled-tube heat exchanger. Cooling in this case was provided by air circulation.

The sample used in the laboratory measurements was a dried limestone cylindrical core. The dimensions were 3.175 cm diameter and 2.54 cm length. The tests begin by bringing the whole apparatus to a constant homogeneous temperature. After leaving the cell in this condition for 2 h, the recording starts and the system is maintained quiescent for another 30 min. The main heater is turned on while the bottom heater is controlled to keep the bottom temperature constant. In the tests reported here, the main heater was programmed to sustain the top temperature also at a constant value. Figures 7 and 8 illustrate the

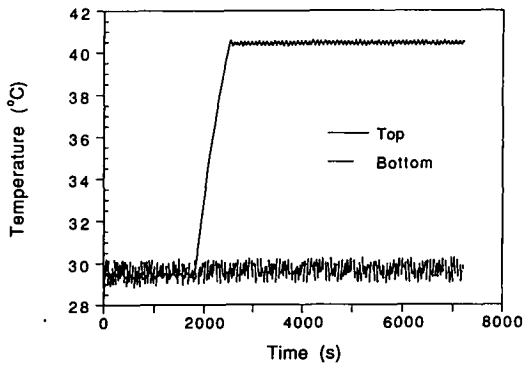

FIG. 7. Temperature history during the experiment.

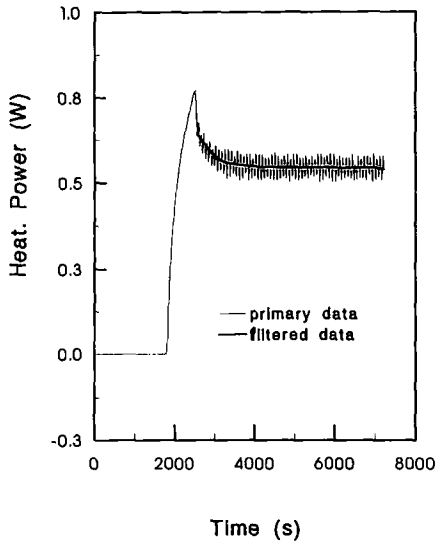

FIG. 8. Heat flux applied at the top surface of the sample.

recordings obtained for the temperatures and the heat fluxes, respectively. The data are plotted as collected. The oscillations in the temperature and heat flux readings are due to the power switching for the control of the system. In the case of heat flux, it started only after the top of the sample reached the desired temperature. In order to proceed with the data treatment, the heat flux data were smoothed out by a filter algorithm based on Fourier transforms [7].

The experimental data were then treated by the techniques explained earlier in the paper. The final treated data are shown on the plots of Figs. 9 and 10, respectively for the determination of diffusivity and conductivity. The number of points on these graphs is irrelevant and there can be as many points as desired. The s range covered by the data is very important. The graph in Fig. 9 shows that below a certain value of $s^{-1/2}$, the data points deviate from the straight line. The reason is the uncertainty brought by the extrapolation to very small values of time. For s values greater than 0.02 ($s^{-1/2}$ less than 7 in the graph) the minimum limit in the Laplace transform must be less

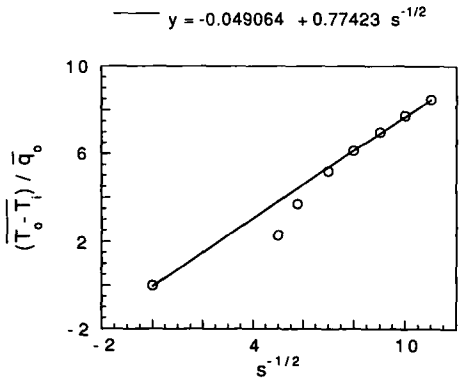

FIG. 9. Early data plot used to estimate diffusivity.

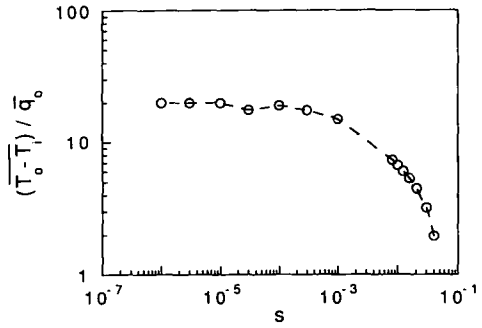

FIG. 10. Long term plot used to determine conductivity.

than 0.5 s for an accuracy better than 1%. In the extreme low limit the theoretical point (0, 0) helps locate the line needed for parameter estimation. For the data set obtained in this example case, the linear fit shown on Fig. 9 yields

$$\beta = 0.774\,\mathrm{K\,W^{-1}\,s^{-1/2}}. \tag{36}$$

The plot on Fig. 10 refers to the steady-state regime. In the lower range, for s values less than 10^{-4}, heat conduction has achieved the steady condition. As pointed out before, at this point the curve levels off to a horizontal line. The offset from the straight line seen at $s = 3 \times 10^{-5}$ drives attention to the error introduced by the upper limit in the Laplace transform. The smaller the value of s, the greater the upper limit must be to render accurate results. In the tests reported here, down to s values of 10^{-4} the upper limit used was 10^4. In the s range below 10^{-4}, the limit was increased to 10^5. For illustration purposes, the offset point in the figure was obtained with an upper limit of 10^4. It is vitally important to count on an appropriate algorithm of extrapolation, if the trend must be confirmed on an experiment that is definitely stabilized but is not run long up to the upper time limit. A well-behaved pattern for both temperature and heat flux history data is also very helpful at this stage. The value obtained in the steady region is

$$\frac{(\overline{T_o - T_i})}{\overline{q_o}} = 19.95 \tag{37}$$

rendering for the conductivity of the sample material the value of $K = 1.59\,\mathrm{W\,m^{-1}\,K^{-1}}$. From these figures the value obtained for the diffusivity is $\alpha = 0.97 \times 10^{-6}\,\mathrm{m^2\,s^{-1}}$.

CONCLUSION

A new transient method is proposed to measure thermal properties, specifically diffusivity and conductivity, in saturated porous material. The numerical procedure needed to treat the data was tested for accuracy against theoretical data and proved to be adequate. The whole method was used to obtain properties in the laboratory from field samples. The time required in the procedure was somewhat long, in the order of the time needed in steady-state methods. This

is due, however, to the fact that the cell used in the experiment was designed for steady-state measurements. This time can be significantly reduced if a smaller sample is used or if diffusivity is the only objective.

Acknowledgements—This study was developed during the term of the first author as Senior Visiting Fellow at University of Texas. Professor Trevisan gratefully acknowledges the hospitality at UT and the support from FAPESP-SP-Brazil. Financial support for this work was provided by USDOE under contract DE-90BC14661.

REFERENCES

1. M. Miller and S. Mohanty, Thermal and Thermo-Mechanical Effects in Thermal Oil Recovery, Center for Enhanced Oil and Gas Recovery Research Annual Report, Category B (1991)
2. R. P. Tye, *Thermal Conductivity*. Academic Press, New York (1969).
3. J. D. Scott and A. C. Seto, Thermal properties measurements on oil sands, *J. Can. Petrol. Technol.* **25,** 70–77 (1970).
4. T. Z. Harmarthy, Variable-state methods of measuring the thermal properties of solids, *J. appl. Phys.* **35,** 1190–1200 (1964).
5. D. C. Shallcross and D. G. Wood, The accurate measurement of heat flux using film heat sensors with application to axisymmetric bodies, *Proceedings of the Eighth International Heat Transfer Conference*, San Francisco, California, Vol. 2, 477–482 (1986).
6. E. W. Cheney and D. Kincaid, *Numerical Mathematics and Computing*. Brooks/Cole, Monterey-CA (1980).
7. W. H. Press, B. P. Flannery, S. A. Teukolsky and W. T. Vetterling, *Numerical Recipes*. Cambridge University Press, Melbourne (1989).
8. H. S. Carslaw and J. C. Jaeger, *Conduction of Heat in Solids*. Oxford University Press, London (1959).
9. H. Stehfest, Algorithm 368, Numerical inversion of Laplace transform, *Communications of the ACM* **13,** 47–49 (1970).